

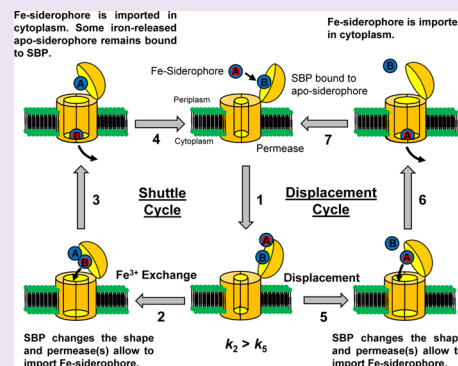
Direct Evidence of Iron Uptake by the Gram-Positive Siderophore-Shuttle Mechanism without Iron Reduction

Tatsuya Fukushima,[†] Benjamin E. Allred,[†] and Kenneth N. Raymond*

Department of Chemistry, University of California, Berkeley, California 94720-1460, United States

S Supporting Information

ABSTRACT: Iron is an essential element for all organisms, and microorganisms produce small molecule iron-chelators, siderophores, to efficiently acquire Fe(III). Gram-positive bacteria possess lipoprotein siderophore-binding proteins (SBPs) on the membrane. Some of the SBPs bind both apo-siderophores (iron-free) and Fe-siderophore (iron-chelated) and only import Fe-siderophores. When the SBP initially binds an apo-siderophore, the SBP uses the Gram-positive siderophore-shuttle mechanism (the SBPs exchange Fe(III) from a Fe-siderophore to the apo-siderophore bound to the protein) and/or displacement mechanism (the apo-siderophore bound to the SBP is released and a Fe-siderophore is then bound to the protein) to import the Fe-siderophore. Previously, we reported that the *Bacillus cereus* SBP, YxeB, exchanges Fe(III) from a ferrioxamine B (FO) to a desferrioxamine B (DFO) bound to YxeB using the siderophore-shuttle mechanism although the iron exchange was indirectly elucidated. Synthetic Cr-DFO (inert metal FO analog) and Ga-DFO (nonreducible FO analog) are bound to YxeB and imported via YxeB and the corresponding permeases and ATPase. YxeB exchanges Fe(III) from FO and Ga(III) from Ga-DFO to DFO bound to the protein, indicating that the metal-exchange occurs without metal reduction. YxeB also binds DFO derivatives including acetylated DFO (apo-siderophore) and acetylated FO (AcFO, Fe-siderophore). The iron from AcFO is transferred to DFO when bound to YxeB, giving direct evidence of iron exchange. Moreover, YxeB also uses the displacement mechanism when ferrichrome (Fch) is added to the DFO:YxeB complex. Uptake by the displacement mechanism is a minor pathway compared to the shuttle mechanism.



All organisms including animals, plants, and pathogenic microorganisms need iron as a cofactor for essential biological processes including oxygen binding, electron transfer, and catalysis.¹ In nature iron is abundant, but the biologically available amount of iron is limited since Fe(III) is insoluble in aqueous solution (10^{-10} M soluble Fe³⁺ at physiological pH).² Bacteria require 10^{-6} M intracellular iron,³ indicating that efficient iron acquisition systems are essential. Some microorganisms have import machineries that import Fe(III) by oxidizing Fe(II), including YwbLMN *Bacillus subtilis*⁴ and Ftr1p/Fet3p *Saccharomyces cerevisiae*,^{5,6} but many microorganisms cannot uptake Fe(III) without a chelator. Instead, many microorganisms have transporters for iron-chelating small molecules, called siderophores, to efficiently import iron.

Any siderophore transport system in Gram-positive bacteria must differ from systems in Gram-negative bacteria because Gram-positive bacteria have one membrane (cytoplasmic membrane) and a thick cell wall, while Gram-negative bacteria have two membranes (outer and cytoplasmic membranes) and a thin cell wall in the periplasmic space. Gram-negative bacteria use transmembrane outer membrane transporters (OMTs) to selectively bind target Fe-siderophores on the cell surface. On the other hand, Gram-positive bacteria use lipoprotein siderophore-binding proteins (SBPs) anchored on the membrane to selectively bind the target Fe-siderophores. Thus, the OMTs and SBPs are a key factor for Fe-siderophore

recognition and import. In Gram-positive bacteria Fe-siderophores are imported to the cytoplasm using a complex of a SBP, permease(s), and an ATPase. Several SBPs bind not only Fe-siderophores but also apo-siderophores.^{7–9} The binding affinity of *Bacillus cereus* FpuA, FatB, or FeuA for the target apo-siderophore is similar to the affinity for the Fe-siderophore.⁸

Two questions about the binding of apo-siderophores to SBPs have arisen. The first question is what is the utility of binding an apo-siderophore? The answer is still not known. One possible answer is that an apo-siderophore bound to a SBP can catch iron from a variety of ferric species. The second question is how is a Fe-siderophore imported when an apo-siderophore is initially bound to the SBP? When an SBP is bound to an apo-siderophore, the SBP can uptake a Fe-siderophore with two different mechanisms. One mechanism is the Gram-positive siderophore-shuttle where the SBPs exchange Fe(III) from a Fe-siderophore to the initially bound apo-siderophore followed by uptake. The other mechanism is the displacement mechanism in which the apo-siderophore initially bound to the SBP is released and a Fe-siderophore is then bound to the protein followed by uptake (Figure 1).⁷ We

Received: April 29, 2014

Accepted: July 9, 2014

Published: July 9, 2014

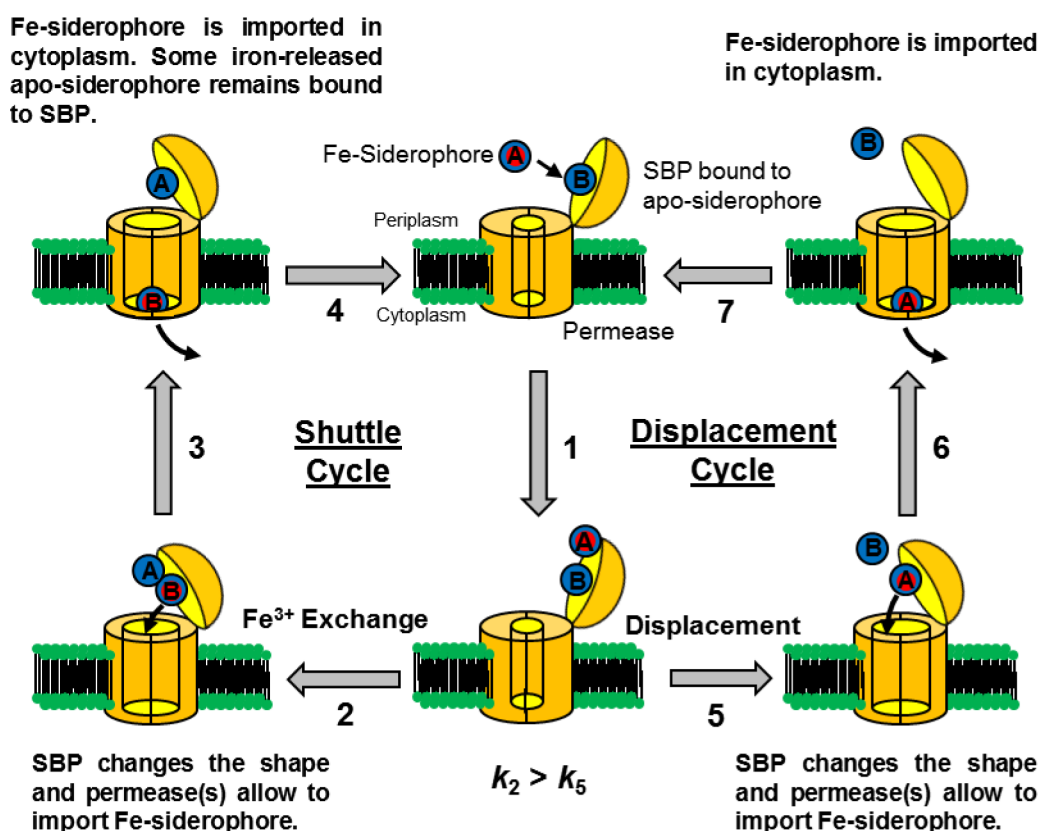


Figure 1. Models of the Gram-positive siderophore-shuttle mechanism and displacement mechanism of YxeB. YxeB is initially bound to an apo-siderophore. (1) A Fe-siderophore approaches YxeB and rests near the binding pocket occupied by the apo-siderophore. At this step two pathways are possible. Steps 2–4 are the shuttle pathway. (2) Iron exchanges from the Fe-siderophore to the apo-siderophore in the binding pocket. The protein facilitates this step by increasing the local concentration of the entering ligand and the ferric complex. (3) The new Fe-siderophore (B) is transported and the created iron-released ligand (A) may remain to be bound to the YxeB protein. (4) The receptor is bound to an apo-siderophore. Steps 5–7 are the displacement pathway. (5) The Fe-siderophore displaces the apo-siderophore and occupies the binding pocket. (6) The original Fe-siderophore (A) is transported. (7) The SBP is bound to an apo-siderophore. In the Gram-positive siderophore-shuttle both pathways operate but the shuttle pathway is preferred.

demonstrated that a *B. cereus* SBP, YxeB, binds the apo- and Fe-siderophores DFO/DFch (desferrichrome) and FO/Fch (ferrichrome), respectively (chemical structures shown in Supporting Information Figure 1). When YxeB is initially bound to an apo-siderophore, it facilitates exchange of iron from a Fe-siderophore to the bound apo-siderophore, thus explaining the efficacy of binding apo-siderophore. Metal exchange is a fundamental step in a siderophore-shuttle import mechanism, and YxeB is the first protein identified to function in a Gram-positive siderophore-shuttle mechanism.⁷

Questions for YxeB and the Gram-positive shuttle mechanism remain. Does YxeB need to reduce Fe(III) of the Fe-siderophore, FO, during the iron exchange process? Does the shuttle provide any advantage over the displacement mechanism? Can YxeB facilitate exchange of iron from other siderophores such as Fe-enterobactin to the apo-siderophore bound to the protein? To address these questions, the FO/Fch import system, YxeB (SBP) and BC_0382 and BC_0381 (permeases renamed FhuB and FhuG) (Supporting Information Figure 2A), have been further studied. The characteristics of YxeB and the Gram-positive siderophore-shuttle have broad application since many Gram-positive bacteria such as *B. subtilis*,⁴ *Staphylococcus aureus*,¹⁰ *Listeria monocytogenes*,¹¹ and *Streptococcus pneumoniae*¹² possess the FO/Fch import systems. We report that YxeB uses the Gram-positive siderophore-shuttle mechanism in preference to the displace-

ment mechanism, and we successfully demonstrate that iron exchanges from a Fe-siderophore to an apo-siderophore bound to the protein without intermediate metal ion reduction.

RESULTS AND DISCUSSION

YxeB Binds Ga-DFO. Previously, the *yxeB* gene in *B. cereus* ATCC 14579 in the laboratory stock was sequenced and the nucleotides contained two variations, TT₄₂₅A (residue 142 is Leu) and TC₄₂₅A (residue 142 is Ser) (the number is with respect to the first nucleotide of the *yxeB* translational start codon).⁷ Although many *B. cereus* strains possess TT₄₂₅A (residue 142 is Leu) in *yxeB*, both variants were used for studying the Gram-positive siderophore-shuttle mechanism.

The natural YxeB variants YxeB-L142-6×His (residue 142 is Leu) and YxeB-S142-6×His (residue 142 is Ser) bind DFO, FO, Fch, DFch, and Cr-DFO.⁷ To further study the metal exchange by YxeB, a new substrate, Ga-DFO, was prepared (chemical structure of DFO is shown in Supporting Information Figure 1A). Gallium(III) cannot be reduced, while iron(III) can be reduced to iron(II), an intermediate in many biological iron transport processes. Hence, Ga-DFO can be used as an irreducible FO analog. The binding ability of the YxeB proteins for Ga-DFO was assessed by a fluorescence quenching assay. The fluorescence of YxeB-L142-6×His was increased instead of quenched by addition of the substrate (Figure 2A). The result is very similar to the fluorescence

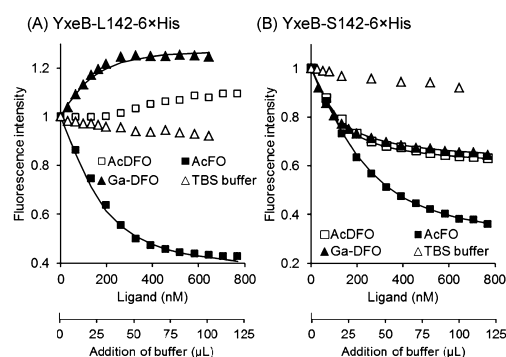


Figure 2. Fluorescence quenching assays of YxeB-L142-6xHis (panel A) and YxeB-S142-6xHis (panel B). The dissociation constants were calculated by Hyperquad²² using the assay data (see Table 1). Open squares, AcDFO; closed squares, AcFO; closed triangle, Ga-DFO; open triangles, TBS buffer (control). The fluorescence quenching curves of YxeB-L142-6xHis for AcFO and Ga-DFO and of YxeB-S142-6xHis for AcFO, AcDFO, and Ga-DFO were fit to the calculated quenching curves (lines) by Hyperquad.²²

enhancement of the protein when binding DFO or DFch,⁷ suggesting that the protein may bind Ga-DFO. The dissociation constant (K_d) of the protein for Ga-DFO is 59.2 nM (Table 1),

Table 1. K_d and Substrate Binding Assay of YxeB-L/S142-6xHis for Several Substrates

substrates	YxeB-L142-6xHis		YxeB-S142-6xHis	
	K_d (nM) by FQ assay	binding assay (HPLC)	K_d (nM) by FQ assay	binding assay (HPLC)
Ga-DFO	59.2 (0.0151 ^a)	bound ^d	44.6 (0.0058 ^a)	bound ^d
AcDFO	NC ^b	bound ^d	30.7 (0.0068 ^a)	bound ^d
AcFO	25.4 (0.0128 ^a)	bound ^d	31.6 (0.0047 ^a)	bound ^d
DFch	103.8 ^c (0.0189 ^a)	bound ^d	23.0 ^c (0.0113 ^a)	bound ^d
Fch	43.0 ^c (0.0184 ^a)	bound ^d	29.3 ^c (0.0096 ^a)	bound ^d

^aNumbers with parentheses are the SDs. ^bNC is not calculated by Hyperquad²² because the fluorescence curve of YxeB-L142-6xHis for AcDFO did not show saturation (Figure 2). ^c K_d for DFch or Fch was calculated using fluorescence quenching data previously described.⁷

^dBound means that substrates are detected in the protein complex analyzed by RP-HPLC (Supporting Information Figures 3 and 4).

and the value is similar to the K_d for FO (38.8 nM).⁷ The fluorescence of YxeB-S142-6xHis for Ga-DFO was quenched (Figure 2B), and the dissociation constant (K_d) is 44.6 nM (Table 1), indicating that the protein binds Ga-DFO like FO, for which the K_d is 29.1 nM.⁷

To confirm binding of Ga-DFO to the YxeB proteins, after the proteins and Ni-agarose beads had been mixed in order to bind the proteins to the beads, Ga-DFO was added in the mixture. The mixture was centrifuged to separate the protein complex binding to the beads (pellet) and unbound solution (supernatant). The bound ligand, Ga-DFO, was separated from the protein complex as described in the Methods and was then quantified by RP-HPLC. As shown in Supporting Information Figure 3B and C, both proteins, YxeB-L/S142-6xHis, contained Ga-DFO. Thus, this result by RP-HPLC confirmed that the YxeB proteins bind Ga-DFO.

YxeB-FhuBG Machinery Can Import Cr- and Ga-DFO.

The gene encoding the DFO/Fch-binding protein, YxeB, makes an operon with the predicted permease genes, *fhuB* and *fhuG* (Supporting Information Figure 2A). The *fhuB* and *fhuG* genes were disrupted (strain TC137) and the iron uptake was assessed by growth assay and disc diffusion assay as described in the Methods. The *B. cereus* ATCC 14579 host strain does not produce DFO and DFch,¹³ indicating that the concentrations of DFO/FO and the DFO analogs, Cr-DFO and Ga-DFO, can be quantitatively controlled by adding the compounds to the culture. The growth assay showed that the growth of the TC137 strain is delayed with DFO or DFch compared to the growth of wild-type strains, TC129 and TC128 (Supporting Information Figure 2B and C). Moreover, the strain did not grow around a disc containing DFO or DFch (Supporting Information Figure 2D), indicating that FhuB and/or FhuG are essential for importing FO and Fch.

To assess whether Ga-DFO and Cr-DFO are actually imported into the cytoplasm, the amount of Ga or Cr in the cells was measured by ICP. The wild-type strains, TC128 and TC129, incubated with the respective metal complex contained Ga or Cr in the cells while TC111 (*yxeB*[−] *fhuB*⁺ *fhuG*⁺) and TC137 (*yxeB*[−] *fhuB*[−] *fhuG*[−]) did not (Figure 3A and B). Since the amount of Ga or Cr in TC137 (with YxeB) was the same as the amount in TC111 (no YxeB) (Figure 3A and B), the Ga and Cr levels of the wild-type strains represent imported metal-siderophore, not metal-siderophore bound at the cell surface by

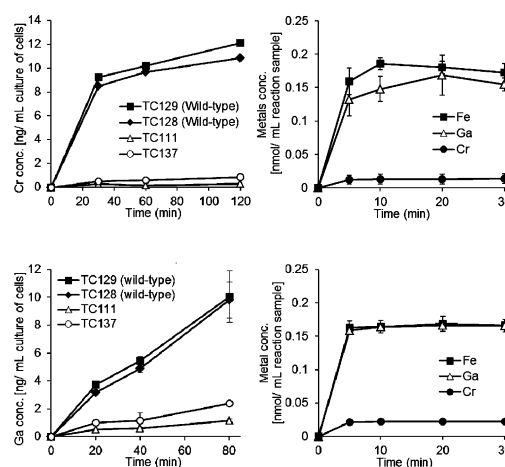


Figure 3. (A and B) Imported Cr amounts (panel A) and Ga amounts (panel B) in cells of TC129 (YxeB-L142, wild-type), TC128 (YxeB-S142, wild-type), TC111 (*yxeB*[−]), and TC137 (*fhuBG*[−]). 2 μ M Cr-DFO or Ga-DFO was added in the culture and the amount of Cr or Ga in the cells was measured by ICP. The optical density (OD) of the cultures at 600 nm after 0 and 120 min incubation with Cr-DFO were 0.9–1.3 and 2.0–2.1, respectively. The OD at 600 nm after 0 and 80 min incubation with Ga-DFO were 0.8–1.1 and 1.6–1.8, respectively. Data are the average of two independent experiments. Bars are the standard errors. (C and D) *In vitro* substrate binding (exchange or displacement) assays for the DFO:YxeB-L/S142-6xHis complex. After the DFO:YxeB-L/S142-6xHis complex had been created, 0.2 μ M FO, Ga-DFO or Cr-DFO was added in the samples. The protein complex was collected as described in the Methods and the amount of Fe, Ga or Cr in the complex was then measured by ICP. Fe amount, closed squares; Ga amount, open triangles; Cr amount, closed circles. Data are the average of three independent experiments. Bars indicate the standard errors. The amount of Fe, Ga, or Cr in the complex after 30 min incubation is shown in Table 2.

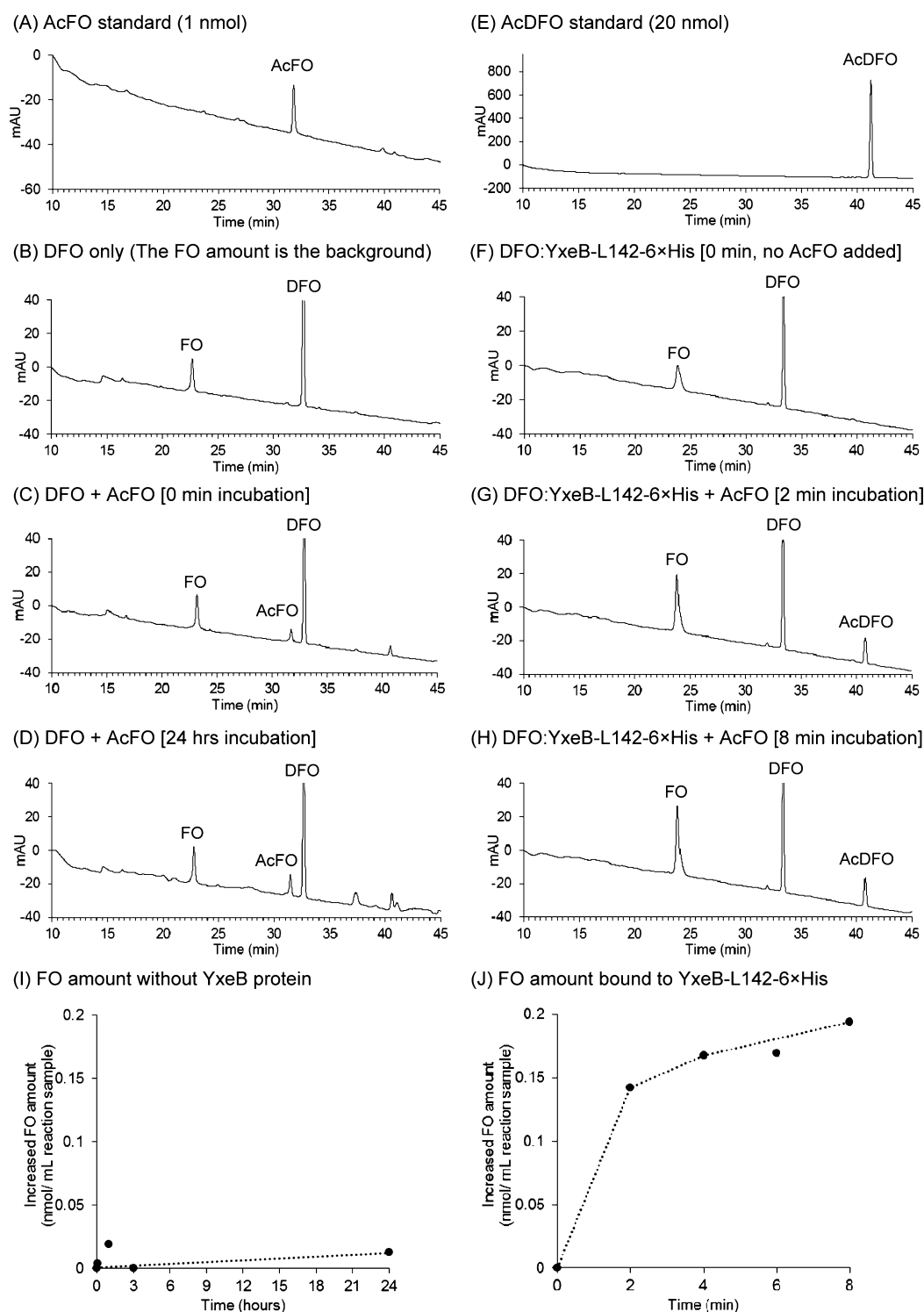


Figure 4. Iron exchange from AcFO (0.2 μ M, final concentration) to DFO (4 μ M, final concentration) with or without YxeB-L142-6xHis (2 μ M, final concentration). The amounts of AcFO, AcDFO, FO, and DFO were assessed by RP-HPLC. (A, B, and E) AcFO (panel A), DFO (panel B), and AcDFO (panel E) standards analyzed by RP-HPLC. As shown in panel B there is a small amount of FO in the DFO standard solution arising from minor iron impurities. (C, D, and I) Amounts of ligands after 0 min and 24 h incubation with AcFO, DFO, and no YxeB were analyzed by RP-HPLC. The amounts of formed FO (iron-transferred DFO from AcFO) after 0, 1, 3, and 24 h incubation without the protein are shown in panel I. (F to H and J) Amount of substrates bound to the protein without AcFO (panel F) and after 2 and 8 min incubation with AcFO (panel G and H) as determined by RP-HPLC. The amount of formed FO that is bound to the protein after 2, 4, 6, and 8 min incubation with AcFO and the DFO:YxeB-L142-6xHis complex are shown in panel J.

YxeB. Thus, the results of the *in vivo* metal uptake studies (Figure 3A and B) show that Ga-DFO and Cr-DFO can be imported via the YxeB-FhuBG machinery.

Fe and Ga from FO and Ga-DFO are Transferred to DFO Bound to YxeB. Ga-DFO is bound to YxeB and imported by *B. cereus* (Figures 2 and 3, Supporting Information

Figure 3, and Table 1). Thus, the substrate can be used as an irreducible FO analog. The substrate binding (exchange or displacement) experiment *in vitro* was performed using FO, Ga-DFO, and Cr-DFO. First the DFO:YxeB complex was formed and confirmed by RP-HPLC (see Figure 4F), and then Ga-DFO, FO, or Cr-DFO was added to the sample. As shown in Figure 3C and D and Table 2, the YxeB complexes contained

Table 2. Substrate Amounts Bound to YxeB by Exchange or Displacement with YxeB:DFO

metal–substrate added to YxeB:DFO [0.2 nmol/mL sample]	substrates bound to YxeB except DFO [nmol/mL sample]
ICP analysis for DFO:YxeB-L142-6×His complex ^a (Figure 3C)	
Ga-DFO	Ga-DFO, 0.155 (78% ^b)
FO	FO, 0.172 (86% ^b)
Cr-DFO	Cr-DFO, 0.014 (7% ^b)
ICP Analysis for DFO:YxeB-S142-6×His Complex ^a (Figure 3D)	
Ga-DFO	Ga-DFO, 0.165 (83% ^b)
FO	FO, 0.166 (83% ^b)
Cr-DFO	Cr-DFO, 0.022 (11% ^b)
RP-HPLC Analysis for DFO:YxeB-L142-6×His Complex (Figure 5 and Supporting Information Figure 6)	
AcFO	FO, 0.153 (77% ^b); AcDFO, 0.110 (55% ^c)
Fe-Ent	FO, 0.011 (≤5% ^b)
Fe-EDTA	FO, 0.003 (≤1% ^b)
Fch	FO, 0 (0% ^b); Fch, 0.037 (19% ^b)
Fe-Cit	FO, 0.089 (45% ^b)
hematin	FO, 0.003 (≤1% ^b)
RP-HPLC Analysis for DFO:YxeB-S142-6×His Complex (Supporting Information Figure 5)	
AcFO	FO, 0.144 (72% ^b); AcDFO, 0.089 (45% ^c)

^aSubstrate amounts bound to YxeB after 30 min incubation of YxeB:DFO with metal–substrate are shown. ^bPercentages are metal exchange rates or displaced substrate rates. ^cPercentages indicate rates of iron-released substrate remaining bound to YxeB.

Ga and Fe (>0.15 nmol/mL reaction solution) but not Cr (≤0.02 nmol/mL reaction solution). If the protein uses the displacement mechanism over the Gram-positive siderophore-shuttle mechanism, the YxeB complexes should contain similar amounts of Ga, Fe, or Cr since the binding affinities of YxeB (especially YxeB-S142-6×His) for Ga-DFO, FO, and Cr-DFO are similar (Table 1). The Cr(III) of Cr-DFO (an inert, nonexchangeable metal complex^{14,15}) was not contained in the DFO:YxeB complexes and the exchangeable metals, Ga(III) and Fe(III), were contained by the complex. The Ga(III) and Fe(III) from Ga-DFO and FO, respectively, are transferred to YxeB-bound DFO by the Gram-positive siderophore-shuttle mechanism. Significantly, the amounts of metal transferred from Ga-DFO and FO after 5 min incubation are 0.14–0.18 nmol/mL reaction solution. Since the final concentration of Ga-DFO or FO added in the assay was 0.2 μM (see Methods), >70% of Ga and Fe are transferred to the DFO:YxeB complex within the 5 min incubation time (Figure 3C and D).

Synthetic AcDFO and AcFO Can Be Used as DFO and FO Analogs. To study the iron exchange by YxeB, acetylated DFO and FO, AcDFO and AcFO, respectively, were synthesized. Since the four compounds, AcDFO, AcFO, DFO, and FO, are separated by RP-HPLC (see Figure 4), they are suitable probes to examine the iron exchange by YxeB. The fluorescence of YxeB-L142-6×His was quenched by binding AcFO similar to FO (Figure 2A), and the calculated

K_d is 25.4 nM (Table 1), which is similar to the K_d for FO (38.8 nM).⁷ Binding by AcDFO increased the fluorescence of YxeB-L142-6×His (Figure 2A). Analysis of a solution of protein and siderophore by RP-HPLC shows that the protein contains AcDFO and AcFO (Supporting Information Figure 4 and Table 1), indicating that both ligands bind to the protein. YxeB-S142-6×His also binds AcDFO and AcFO such as DFO and FO, respectively, since the fluorescence was quenched by addition of AcDFO or AcFO (Figure 2B). The calculated K_d values for AcDFO and AcFO were 30.7 and 31.6 nM, respectively (Table 1), similar to the K_d values for DFO (35.9 nM) and FO (29.1 nM) calculated previously.⁷ Additionally, the complex analysis by RP-HPLC demonstrates that the protein–substrate complex contained AcDFO and AcFO (Supporting Information Figure 4 and Table 1). Thus, AcDFO and AcFO can be used as DFO and FO analogs.

Iron Is Transferred from AcFO to DFO by YxeB (“Direct Evidence” Of Iron Transfer by YxeB). To study the iron exchange by YxeB, after the DFO:YxeB complexes had been created, synthesized AcFO was added to the sample. After the addition, both YxeB proteins, YxeB-L142-6×His and -S142-6×His, contained FO (Figures 4G and H, 5B [YxeB-L142-6×His] and Supporting Information Figure 5 [YxeB-S142-6×His]). Since AcFO was the only iron source added to the solution of DFO:YxeB complex, the increased amount of iron observed in the protein-siderophore complex comes from AcFO. Thus, this result is strong evidence that the iron is transferred from AcFO to DFO:YxeB. Remarkably, the protein complexes also contained AcDFO, the iron-depleted substrate, clearly indicating that the iron-released substrate after iron exchange remains bound to YxeB.

Iron exchange between AcFO and DFO did not occur without YxeB even after 24 h (Figure 4C, D, and I). On the other hand, the iron exchange with YxeB was complete after only 2 min incubation (Figure 4G), and the exchange amount after 8 min incubation was approximately 0.2 μM (0.2 nmol/mL reaction sample) FO (Figure 4J). Since the AcFO added to the sample gave a final concentration of 0.2 μM, Figure 4J clearly shows that almost all iron (0.2 μM, final concentration) from AcFO is immediately transferred to DFO bound to YxeB.

Iron Cannot Be Transferred from Several Iron-Chelators to DFO Bound to YxeB. YxeB transfers iron from FO or AcFO to DFO bound to the protein. However, it is not known whether the protein can obtain iron from the other iron-chelators. Several iron-chelators including Fe-enterobactin (Fe-Ent, pFe^{III} = 34.3),¹⁶ AcFO (pFe^{III} for DFO = 26.6),¹⁷ Fch (pFe^{III} = 25.2),¹⁸ Fe-EDTA (pFe^{III} = 23.4),¹⁹ hematin, and Fe/citrate (the ligand should be FeCit₂ as the predominant species [Supporting Information Figure 6C]) were used for the iron-exchange assays. As shown in Figure 5, Supporting Information Figure 6 and Table 2 the iron of AcFO or FeCit₂ (weak iron-chelator) was transferred to the DFO:YxeB complex, while the iron of the other ligands, Fe-Ent, Fe-EDTA, or hematin, was not. Thus, the iron exchange does not occur between DFO and the other chelators except FeCit₂. Iron transfer does not depend solely on the stability of the potential iron donor because the iron from Fe-EDTA is not transferred to the complex. Iron exchange to the DFO:YxeB complex may also depend on the ability of the Fe-chelators to fit in a binding pocket of YxeB.

The analysis of YxeB and DFch or Fch by RP-HPLC shows that YxeB binds DFch and Fch (Supporting Information Figure 3D–I). The iron of Fch was not transferred; however, a small

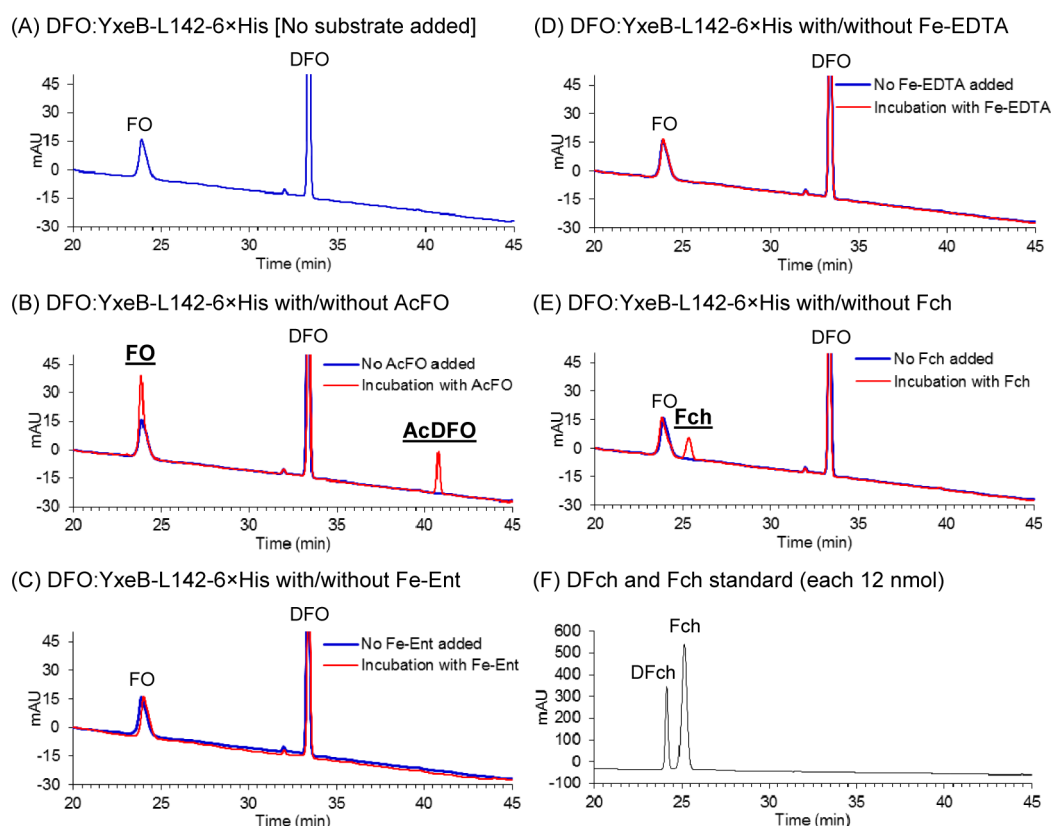


Figure 5. Iron exchange from Fe-siderophores or iron-chelators to the DFO:YxeB-L142-6xHis complex. (A to E) After 4 μ M DFO and 2 μ M the YxeB protein had been mixed to create the DFO:YxeB complex, 0.2 μ M AcFO (panel B), Fe-Ent (panel C), Fe-EDTA (panel D), or Fch (panel E) was added to the sample. The complex without substrate addition (blue chromatograph) and the complex after 40 min incubation with the substrate (red chromatograph) were collected and analyzed by RP-HPLC. Peaks with the thick and underlined letters are the increased products. The calculated amount of compounds bound to the protein is shown in Table 2. (F) RP-HPLC analysis of DFch and Fch standards.

amount of Fch was bound to YxeB (Figure 5E). The bound Fch is due to the displacement mechanism, and the amount of Fch bound to the protein was 0.037 μ M (Table 2). Since 0.2 μ M Fch was used for the iron exchange experiment (see Methods), less than 20% of Fch was bound to the protein after 40 min incubation. Thus, YxeB uses the displacement mechanism for the Fch binding, although this mechanism is less efficient than the Gram-positive siderophore-shuttle mechanism.

YxeB Uses the Gram-Positive Siderophore-Shuttle Mechanism in Preference to the Displacement Mechanism When Apo-Siderophore Is Present. When DFO is initially bound to YxeB, very little Cr-DFO binds to the protein by displacing the apo-siderophore (the displacement mechanism) (Figure 3C and D and Table 2) and only a small amount of the DFO is displaced by Fch (Figure 5E and Table 2). On the other hand, the iron from FO or AcFO is immediately transferred to DFO bound to YxeB within 5 min by iron exchange (Figures 3 and 4) (the Gram-positive siderophore-shuttle mechanism). These *in vitro* experiments clearly show that the DFO:YxeB-L/S142 complex accumulates metal-siderophore by metal exchange, diagnostic of the Gram-positive siderophore-shuttle mechanism, over the displacement mechanism.

The *in vivo* Cr-DFO import experiment shows that the K_m of Cr-DFO import by the TC129 strain (wild-type) without DFO is two times smaller than the K_m with 2 μ M DFO (to make the DFO:YxeB complex), and the V_{max} without DFO is two times higher than the V_{max} with 2 μ M DFO (Table 3). The kinetic

Table 3. Kinetics of Cr-DFO Import by TC129^a

ligand	K_m (μ M)	V_{max} (pmol Cr mL ⁻¹ min ⁻¹)	V_{max}/K_m
Cr-DFO only	0.74 (0.19)	3.11 (0.36)	4.20
Cr-DFO + 2 μ M DFO (DFO:YxeB-L142 complex initially formed)	1.59 (0.17)	1.82 (0.28)	1.14

^aNumbers with parentheses are the standard errors.

value, V_{max}/K_m , with DFO is four times lower than the V_{max}/K_m without DFO (Table 3), indicating that the Cr-DFO is less efficiently imported when the DFO:YxeB complex is initially formed. Thus, the presence of apo-siderophore inhibits metal uptake when the shuttle mechanism is blocked by an inert metal. The displacement mechanism is an inefficient metal uptake mechanism when apo-siderophore is initially bound.

The kinetic observations taken together with the metal exchange experiments show the advantage of the shuttle mechanism over the displacement mechanism. Siderophores are secreted from the cell surface during growth in iron-limited conditions, and apo-siderophore concentration is highest near the cell surface. It is probable that SBPs with affinity for apo-siderophores, such as YxeB, are occupied, which would inhibit iron uptake if metal exchange to the bound apo-siderophore did not take place. In this situation, ferric siderophore is more efficiently acquired via the shuttle mechanism, facilitated by the YxeB, than by the displacement mechanism.

We suggest that the FO/Fch-binding proteins in many Gram-positive bacteria might use the Gram-positive siderophore-shuttle and the displacement mechanisms described here if they can bind apo- and Fe-siderophores. Having SBPs with the two mechanisms enables the bacteria to obtain iron not only from the target Fe-siderophores but also from free iron and weak iron-chelators. Finally, the iron acquisition mechanism of YxeB differs from the siderophore-shuttle mechanism in Gram-negative bacterium, *Aeromonas hydrophila*, in that the *A. hydrophila* siderophore-shuttle protein uses only the iron-exchange mechanism.^{20,21}

METHODS

Information for all plasmids and strains used in the study is shown in Supporting Information Table 1 and the method of construction of a *B. cereus fhuBG* markerless mutant is shown in the Supporting Information.

Fluorescence Quenching Assays of YxeB-L/S142-6×His for Synthesized Ga-DFO, AcDFO, and AcFO. Fluorescence quenching assays of YxeB-L/S142-6×His for the Ga-DFO, AcDFO, and AcFO were performed as described previously.⁷ The dissociation constants were calculated by Hyperquad.²²

YxeB-L/S142-6×His Binding Assay for Ga-DFO, DFch, Fch, AcDFO, and AcFO Using RP-HPLC (Reverse-Phase High Performance Liquid Chromatography). The binding assay was described previously.⁷ The YxeB-L/S142-6×His protein (2 μ M, final concentration) and 50 μ L of Ni Sepharose 6 Fast Flow agarose beads (Ni-agarose beads) (GE Healthcare) were mixed in 5 mL of TBS buffer and the mixture was then gently shaken for 2 h at RT to make the YxeB-L/S142-6×His:Ni-agarose beads complex. The substrate, 10 μ M Ga-DFO, Fch or AcFO, or 20 μ M DFch or AcDFO, was added in the sample and the mixture was then gently shaken for 10 min at RT, followed by centrifuging the sample. The pellet containing the complex was washed by TBS buffer twice.

For the Ga-DFO samples, AcCN (400 μ L of 20% (v/v)) was added in the pellet containing YxeB, and the sample was then kept at RT for 20 min, followed by centrifuge of the samples. After the supernatant had been collected, 1600 μ L of Milli-Q was added in the samples and the samples were filtered. The samples were analyzed by RP-HPLC with a Luna 5 μ C18 column (150 \times 4.60 mm 5 μ m, Phenomenex) to determine whether the protein binds the substrates or not (flow rate, 1 mL/min; monitoring wavelength 220 nm). Elution buffer A and B for the RP-HPLC are 20 mM ammonium acetate (pH 5.5) and 100% (v/v) CH₃CN, respectively. The elution was performed for 50 min with a linear gradient of 0% to 25% buffer B.

For the DFch, Fch, AcDFO, and AcFO samples, 1 mL of 0.1% (v/v) TFA was added in the samples and the samples were kept at RT for 20 min, followed by filtration of the samples. The samples were analyzed by RP-HPLC with a Luna 5 μ C18 column (150 \times 4.60 mm 5 μ m, Phenomenex; flow rate, 1 mL/min; monitoring wavelength 220 nm). Elution buffer A and B for the RP-HPLC are 0.1% (v/v) TFA and 100% (v/v) CH₃CN, respectively. The elution was performed for 50 min with a linear gradient of 0% to 25% buffer B.

Growth Assays of TC111 and TC137. Growth assays were performed as described previously.⁷ In the experiment 10 or 100 nM DFO or DFch was added in iron-limited minimum medium (5 g/L glucose, 3 g/L Difco bacto casamino acid, 1 g/L [NH₄]₂HPO₄, 2.5 g/L K₂HPO₄, 2.5 g/L KH₂PO₄, 40 μ M nicotinic acid, 100 μ M thiamine, 36 μ M MnSO₄, 0.3 μ M ZnSO₄, 830 μ M MgSO₄, and 0.05 g/L tryptophan).²³

Disc Diffusion Assays of TC111 and TC137. Disc diffusion assays were performed as described previously.^{7,9} In the experiment 10 nmol of DFO, DFch, or bacillibactin (BB) or 6 μ L of DMSO as the negative control was infused in a sterilized filter.

Measurement of Cr-DFO and Ga-DFO Import in Wild-Type, TC111, and TC137. Cr-DFO and Ga-DFO import assays were performed, as described previously.⁷ In the experiment, 2 μ M Cr-DFO or Ga-DFO was added in the culture.

Since the Cr-DFO imported by the YxeB-FhuBG in the cytoplasm is the product (P), the added Cr-DFO in the culture is the substrate (S) and the YxeB-FhuBG system is like enzyme (E), the Cr-DFO import rate by the YxeB-FhuBG system can be considered as an enzymatic reaction ($E + S \leftrightarrow ES \rightarrow E + P$).^{8,23} For calculating the kinetics parameters, V_{\max} and K_m , of the Cr-DFO import, Cr-DFO (several concentrations) was added to the culture after 0 or 2 μ M DFO had been added in the culture and the sample had been incubated for 15 min at 37 °C. The values of imported Cr amounts for 20 min incubation at 37 °C were used for determining the initial rates since the import amounts are constant within 20 min.⁷ The V_{\max} and K_m were calculated with Excel.

Fe-/Ga-/Cr-DFO Substrate Binding (Exchange or Displacement) Assay In Vitro Using ICP. The exchanged or displaced amounts of Fe, Ga and Cr ions bound to the YxeB proteins were measured using ICP (inductively coupled plasma). DFO (4 μ M, final concentration), 2 μ M YxeB-L142-6×His or YxeB-S142-6×His (final concentration), and 200 μ L Ni Sepharose 6 Fast Flow agarose beads (Ni-agarose beads, GE Healthcare) were mixed in 26 mL of TBS buffer (25 mM Tris-HCl, 3.2 g/L NaCl, 0.08 g/L KCl, [pH 7.4]) and the mixture was gently shaken for 2 h at RT to create the DFO:YxeB complex. After 5 mL of the mixture had been collected and centrifuged, the pellet was collected (0 min sample). Purified 0.2 μ M FO, Ga-DFO, or Cr-DFO (final concentration) was added in the sample and the mixture was incubated at RT. After 5, 10, 20, and 30 min incubation, 5 mL of the mixture was collected and centrifuged, followed by collection of the pellet (5, 10, 20, and 30 min samples). Nitric acid (2.5 mL of 3.5% (v/v)) was added into the samples and the mixtures were kept overnight. After 0.1 ppm Eu had been added as an internal control and the samples had been filtered, the amount of Fe, Ga or Cr was measured by ICP.

Iron Exchange Experiment with or without the YxeB Protein In Vitro. DFO (4 μ M, final concentration), 2 μ M YxeB-L/S142-6×His (final concentration), and 200 μ L of Ni-agarose beads were mixed in 15 mL of TBS buffer for 2 h at RT. After 0.2 μ M AcFO (final concentration) had been added in the sample, 2 mL of the sample was collected and then centrifuged. The pellet containing the protein complex was washed with TBS buffer twice and the YxeB-L/S142-6×His and its substrates were eluted by addition of 2 mL of 0.01% (v/v) TFA for 20 min at RT. The elution was filtered and the sample was then analyzed by RP-HPLC using a Luna 5 μ C18 column (150 \times 4.60 mm 5 μ m, Phenomenex; flow rate, 1 mL/min; monitoring wavelength 220 nm). The elution buffer A of RP-HPLC is 0.1% (v/v) TFA and the buffer B is 100% (v/v) AcCN. The elution was performed for 50 min with a linear gradient of 0% to 25% buffer B.

For the iron exchange experiment without the YxeB protein, 4 μ M DFO (final concentration) and 0.2 μ M AcFO (final concentration) were mixed in 15 mL of TBS buffer and 2 mL of the mixture was then collected at 0 min, 5 min, 1 h, 3 and 24 h incubation at RT. The sample was immediately analyzed by RP-HPLC, as described above.

Iron Exchange Experiment with Several Iron-Chelators or Fe-Siderophores In Vitro. DFO (4 μ M, final concentration), 2 μ M YxeB-L142-6×His (final concentration), and 300 μ L of Ni-agarose beads were mixed in 11 mL of TBS buffer, and the mixture was gently shaken for 2 h at RT. After 5 mL of the mixture had been collected and centrifuged, the pellet was collected ("No substrate added" sample). Equal amounts (20 μ M) of FeCl₃ and iron-chelator/apo-siderophores (DFch, EDTA or apo-Ent) were mixed in TBS buffer [pH 7.4] and the sample was then kept for 2 h to form the ferric complexes Fch, Fe-EDTA, and Fe-Ent. For ferric citrate solution after 20 μ M FeCl₃ and 4 mM citrate (Fe/citrate = 1:200) had been mixed and the pH of the solution was adjusted at pH 7, the sample was kept for 2 h. Equilibrated iron-substrate (0.2 μ M Fch, Fe-EDTA, or Fe-Ent, final concentration), AcFO (0.2 μ M, final concentration), or hematin (Sigma-Aldrich) (0.2 μ M, final concentration) was added in the sample. Equilibrated ferric citrate was also added in the sample (Fe/citrate = 0.2 μ M: 40 μ M, final concentration). In the final concentration FeCit₂ is a main component (Supporting Information Figure 6C) and the speciation diagram of ferric citrate shown in Supporting Information Figure 6C was generated by HySS,²⁴ as

described previously²⁵ using values of stability constants ($\log \beta$) for ferric citrate,²⁶ pK_a values of citrate^{27,28} and iron hydroxide formation constants.^{26,29} Reaction sample (5 mL) was collected and centrifuged after 40 min incubation and the pellet was then collected ("Incubation with substrate" sample). The samples were analyzed by RP-HPLC as described above (see "Iron exchange experiment with or without the YxeB protein *in vitro*", the section in Methods).

Synthesis and Purification of FO, Cr-DFO, Ga-DFO, AcDFO, and AcFO. FO was synthesized and purified, as described previously.⁷ Cr-DFO was synthesized and purified using the procedure of Leong and Raymond.³⁰

Ga-DFO was synthesized as follows: Ga(acac)₃ (0.18 g, 0.5 mmol), desferrioxamine methanesulfonate (0.30 g, 0.45 mmol), and KOH (0.11 g, 1.83 mmol) were stirred in methanol overnight. Water was added and the solution was acidified with HCl(aq). The solvent was removed and the residue was dissolved in MeOH/EtOH. A white precipitate formed which was removed by filtration. The precipitation and filtration were repeated to give the title compound (0.219 g, 76% yield): ESI-MS (positive mode) m/z calcd for (M+H) C₂₅H₄₆N₆O₈Ga 627.2627, found 627.2625; Anal. Calcd (Found) for C₂₅H₄₅N₆O₈Ga·HCl·KCl·2H₂O·2MeOH: C, 38.67 (38.42); H, 6.97 (6.91); N, 10.02 (10.10).

AcDFO was synthesized following the procedure of Ihnat et al.³¹ The ¹H NMR spectrum matches the literature characterization. ESI-MS (pos. mode) for C₂₇H₅₁O₉N₆ (M+H) calcd for 603.3712, found 603.3719; anal. calcd (found) for C₂₇H₅₀N₆O₉: C, 53.80 (53.86); H, 8.36 (8.35); N, 13.94 (13.97).

AcFO was synthesized as follows: AcDFO (0.15 g, 0.25 mmol) was dissolved in H₂O and KOH (0.08 g, 1.5 mmol). FeCl₃ (0.04 g, 0.27 mmol) was added to the solution, and the dark red solution was stirred at RT for 36 h. Washed two times with ethyl acetate and one time with CH₂Cl₂. Filtered the aqueous layer to break an emulsion. Washed the aqueous layer two more times with CH₂Cl₂. Removed water and dissolved the residue in methanol. Cooled the solution and filtered off colorless salt. Purified the red solution with columns of Na⁺ exchange resin, BioGel, and cellulose powder. Removed solvent to give a dark red solid (0.1 g, 0.15 mmol, 61% yield): ESI-MS (pos. mode) for C₂₇H₄₈O₉N₆ (M+H) calcd for 656.2832, found 656.2820; anal. calcd (found) for C₂₇H₄₇N₆O₉Fe·2CH₃OH·H₂O: C, 47.22 (47.34); H, 7.79 (7.65); N, 11.39 (11.40).

■ ASSOCIATED CONTENT

● Supporting Information

Supplemental figures and methods. This material is available free of charge via the Internet at <http://pubs.acs.org>.

■ AUTHOR INFORMATION

Corresponding Author

*Phone: 510-642-7219. Fax: 510-486-5283. Email: raymond@socrates.berkeley.edu.

Author Contributions

[†]T.F. and B.E.A. contributed equally to this work.

Notes

The authors declare no competing financial interest.

■ ACKNOWLEDGMENTS

We thank Dr. J. Xu for setting up reverse-phase HPLC; Dr. E. Kreimer for helping with inductively coupled plasma analysis; Prof. J. A. Hoch and Prof. M. Perego for gifting the pBKJ223 plasmid. This work is supported by National Institutes of Health Grants AI11744 (to K.N.R.).

■ REFERENCES

(1) Byers, B. R., and Arceneaux, J. E. L. (1998) *Metal Ions in Biological Systems* (Sigel, A., and Sigel, H., Eds.) Vol. 35, pp 37–66, Marcel Dekker, Inc., New York.

(2) Boukhalfa, H., and Crumbliss, A. L. (2002) Chemical aspects of siderophore mediated iron transport. *Biomaterials* 15, 325–339.

(3) Braun, V., Hantke, K., and Koster, W. (1998) *Metal Ions in Biological Systems* (Sigel, A., and Sigel, H., Eds.) Vol. 35, pp 67–145, Marcel Dekker, Inc., New York.

(4) Ollinger, J., Song, K. B., Antelmann, H., Hecker, M., and Helmman, J. D. (2006) Role of the fur regulon in iron transport in *Bacillus subtilis*. *J. Bacteriol.* 188, 3664–3673.

(5) Singh, A., Severance, S., Kaur, N., Wiltse, W., and Kosman, D. J. (2006) Assembly, activation, and trafficking of the Fet3p.Ftr1p high affinity iron permease complex in *Saccharomyces cerevisiae*. *J. Biol. Chem.* 281, 13355–13364.

(6) Kwok, E. Y., Severance, S., and Kosman, D. J. (2006) Evidence for iron channeling in the Fet3p-Ftr1p high-affinity iron uptake complex in the yeast plasma membrane. *Biochemistry* 45, 6317–6327.

(7) Fukushima, T., Allred, B. E., Sia, A. K., Nichiporuk, R., Andersen, U. N., and Raymond, K. N. (2013) Gram-positive siderophore-shuttle with iron-exchange from Fe-siderophore to apo-siderophore by *Bacillus cereus* YxeB. *Proc. Natl. Acad. Sci. U.S.A.* 110, 13821–13826.

(8) Zawadzka, A. M., Abergel, R. J., Nichiporuk, R., Andersen, U. N., and Raymond, K. N. (2009) Siderophore-mediated iron acquisition systems in *Bacillus cereus*: Identification of receptors for anthrax virulence-associated petrobactin. *Biochemistry* 48, 3645–3657.

(9) Zawadzka, A. M., Kim, Y., Maltseva, N., Nichiporuk, R., Fan, Y., Joachimiak, A., and Raymond, K. N. (2009) Characterization of a *Bacillus subtilis* transporter for petrobactin, an anthrax stealth siderophore. *Proc. Natl. Acad. Sci. U.S.A.* 106, 21854–21859.

(10) Sebulsky, M. T., and Heinrichs, D. E. (2001) Identification and characterization of *fhuD1* and *fhuD2*, two genes involved in iron-hydroxamate uptake in *Staphylococcus aureus*. *J. Bacteriol.* 183, 4994–5000.

(11) Xiao, Q., Jiang, X., Moore, K. J., Shao, Y., Pi, H., Dubail, I., Charbit, A., Newton, S. M., and Klebba, P. E. (2011) Sortase independent and dependent systems for acquisition of haem and haemoglobin in *Listeria monocytogenes*. *Mol. Microbiol.* 80, 1581–1597.

(12) Pramanik, A., and Braun, V. (2006) Albomycin uptake via a ferric hydroxamate transport system of *Streptococcus pneumoniae* R6. *J. Bacteriol.* 188, 3878–3886.

(13) Hotta, K., Kim, C. Y., Fox, D. T., and Koppisch, A. T. (2010) Siderophore-mediated iron acquisition in *Bacillus anthracis* and related strains. *Microbiology* 156, 1918–1925.

(14) Cotton, F. A., and Wilkinson, G. (1988) *Advanced Inorganic Chemistry: A Comprehensive Text*, pp 1283–1334, John Wiley and Sons, New York.

(15) Leong, J., and Raymond, K. N. (1975) Coordination isomers of biological iron transport compounds, IV, Giometrical isomers of chromic desferrioxamine B. *J. Am. Chem. Soc.* 97, 293–296.

(16) Loomis, L. D., and Raymond, K. N. (1991) Solution equilibria of enterobactin and metal–enterobactin complexes. *Inorg. Chem.* 30, 906–911.

(17) Schwarzenbach, G., and Schwarzenbach, K. (1963) Hydroxamatkomplexe I. Die Stabilität der Eisen(III)-Komplexe einfacher Hydroxamsäuren und des ferrioxamins B. *Helv. Chim. Acta* 46, 1390–1400.

(18) Wong, G. B., Kappel, M. J., Raymond, K. N., Matzanke, B., and Winkelman, G. (1983) Coordination chemistry of microbial iron transport compounds. 24. Characterization of coprogen and ferricrocin, two ferric hydroxamate siderophores. *J. Am. Chem. Soc.* 105, 810–815.

(19) Abergel, R. J., Zawadzka, A. M., and Raymond, K. N. (2008) Petrobactin-mediated iron transport in pathogenic bacteria: Coordination chemistry of an unusual 3,4-catecholate/citrate siderophore. *J. Am. Chem. Soc.* 130, 2124–2125.

(20) Stintzi, A., Barnes, C., Xu, J., and Raymond, K. N. (2000) Microbial iron transport via a siderophore shuttle: A membrane ion transport paradigm. *Proc. Natl. Acad. Sci. U.S.A.* 97, 10691–10696.

(21) Szuromant, H., Fukushima, T., and Hoch, J. A. (2007) The essential YycFG two-component system of *Bacillus subtilis*. *Methods Enzymol.* 422, 396–417.

- (22) Gans, P., Sabatini, A., and Vacca, A. (1996) Investigation of equilibria in solution. Determination of equilibrium constants with the HYPERQUAD suite of programs. *Talanta* 43, 1739–1753.
- (23) Dertz, E. A., Stintzi, A., and Raymond, K. N. (2006) Siderophore-mediated iron transport in *Bacillus subtilis* and *Corynebacterium glutamicum*. *J. Biol. Inorg. Chem.* 11, 1087–1097.
- (24) Alderighi, L., Gans, P., Ienco, A., Peters, D., Sabatini, A., and Vacca, A. (1999) Hyperquad simulation and speciation (HySS): A utility program for the investigation of equilibria involving soluble and partially soluble species. *Coord. Chem. Rev.* 184, 311–318.
- (25) Fukushima, T., Sia, A. K., Allred, B. E., Nichiporuk, R., Zhou, Z., Andersen, U. N., and Raymond, K. N. (2012) *Bacillus cereus* iron uptake protein fishes out an unstable ferric citrate trimer. *Proc. Natl. Acad. Sci. U.S.A.* 109, 16829–16834.
- (26) Silva, A. M., Kong, X., Parkin, M. C., Cammack, R., and Hider, R. C. (2009) Iron(III) citrate speciation in aqueous solution. *Dalton Trans.* 40, 8616–8625.
- (27) Martell, A. E., and Smith, R. M. (1977) *Critical Stability Constants* Vol. 3, pp 161, Plenum Press, New York.
- (28) Silva, A. M., Kong, X., and Hider, R. C. (2009) Determination of the pK_a value of the hydroxyl group in the α -hydroxycarboxylates citrate, malate, and lactate by ^{13}C NMR: Implications for metal coordination in biological systems. *Biometals* 22, 771–778.
- (29) Baes, C. F., and Mesmer, R. E. (1976) *The Hydrolysis of Cations*, 1st ed.; pp 226–237, Wiley, New York.
- (30) Leong, J., and Raymond, K. N. (1975) Coordination isomers of biological iron transport compounds. IV. Geometrical isomers of chromic desferrioxamine B. *J. Am. Chem. Soc.* 97, 293–296.
- (31) Ihnat, P. M., Vennerstrom, J. L., and Robinson, D. H. (2000) Synthesis and solution properties of deferoxamine amides. *J. Pharm. Sci.* 89, 1525–1536.